ANALYSIS OF METAMATERIAL ATTACHMENT FOR EM ABSORPTION IN HUMAN HEAD

Mohammad Rashed Iqbal Faruque[1], Mohammad Tariqul Islam[2], Norbahiah Misran[1, 2]

[1]Dept. of Electrical, Electronic and Systems Engineering, Faculty of Engineering and Built Environment, Universiti Kebangsaan Malaysia, Selangor, Malaysia.
[2]Institute of Space Science (ANGKASA), Universiti Kebangsaan Malaysia, Selangor, Malaysia.

Key words: antenna, human head model, lossy-Drude model, metamaterials, specific absorption rate (SAR).

Abstract: The reducing specific absorption rate (SAR) with metamaterials attachment is investigated in this paper. The finite-difference time-domain method with lossy-Drude model is adopted in this analysis. The technique of SAR reduction is discussed and the effects of attaching location, distance, and size of metamaterials, perfect electric conductor (PEC), and materials on the SAR reduction are investigated. Metamaterials have achieved a 41.47% reduction of the initial SAR value for the case of 1 gm SAR. These results suggest a guideline to choose various types of metamaterials with the maximum SAR reducing effect for a phone model.

Vpliv dodatka metamateriala na absorpcijo EM valovanja v človeški glavi

Kjučne besede: antena, model človeške glave, lossy-Drude model, metamateriali, specifična absorbcijska stopnja (SAR)

Izvleček: v članku opišemo zmanjšanje parametra SAR (specifična absorbcijska stopnja) z dodatkom metamateriala. Analizo smo opravili z modelom Drude in uporabo končnih diferenc v časovni domeni. Opisana je tehnika zmanjšanja parametra SAR , raziskani so vpliv lokacije, oddaljenosti in velikosti metamaterialov ter vpliv popolnega električnega prevodnika (PEC) in vrste metamaterialov na zmanjšanje SAR. Z uporabo metamaterialov smo dosegli 41,47 % zmanjšanje začetne vrednosti SAR, ki je bila 1gm SAR. Ti rezultati pomenijo neko vrsto smernic za izbiro materialov za mobilne telefone, ki najbolj zmanjšujejo parameter SAR.

1. Introduction

With the rapid and ever more widespread use of mobile phones, public concern regarding the possible health hazards has been growing, which brings an increased requirement on electromagnetic (EM) absorption for mobile phones. The basic parameter in the EM absorption is defined in terms of the specific absorption rate (SAR), or the absorbed power in unit mass of tissue /1/. The SAR is generally evaluated using either phantom measurement or computer simulation. The finite-difference time-domain (FDTD) method is currently the most widely accepted means for the SAR computations /2/. The interaction of handset antennas with the human body is a great consideration in cellular communications. The user's body, especially the head and hand, influence the antenna voltage standing wave ratio (VSWR), gain, and radiation patterns. Furthermore, thermal effects, when tissues are exposed to unlimited electromagnetic energy, can be a serious health hazard. Therefore standards organizations have set exposure limits in terms of SAR /3, 4/. SAR is a measure of the rate at which radio frequency (RF) energy is absorbed by the body when exposed to a radio-frequency electro-magnetic field. SAR is used to measure exposure to fields between 100 kHz and 10 GHz /5-8/. It is commonly used to measure power absorbed from mobile phones and during MRI scans. The value will depend on the geometry of the part of the body that is exposed to the RF energy, and on the exact location and geometry of the RF source. Cellular phone protection and the enforcement of pertinent exposure standards are issues in the current media, and regulatory agencies are motivated to assure that compliance testing is acceptable. IEEE Standard 1528 /3/ and IEC 62209-1 specify protocols and process for the measurement of the peak spatial-average SAR induced inside a simplified model of the head of users of hand held radio transceivers (cellular phones). For example, the SAR limit specified in IEEE C95.1: 1999 is 1.6 W/kg in a SAR 1 gm averaging mass while that specified in IEEE C95.1: 2005 has been updated to 2 W/kg in a 10 gm averaging mass /4/. This new SAR limit specified in IEEE C95.1: 2005 is comparable to the limit specified in the International Commission on Non-Ionizing Radiation Protection (ICNIRP) guidelines.

The interaction of the cellular handset with the human head has been investigated by many published papers considering; first, the effect of the human head on the handset antenna performance including the feed-point impedance, gain, and efficiency /7-9/, and second, the impact of the antenna EM radiation on the user's head due to the absorbed power, which is measured by predicting the induced SAR in the head tissue /10-13/.

The most used method to solve the electromagnetic problem in this area is the finite-difference time-domain (FDTD) technique /13-14/. Although, in principle, the solution for general geometries does not require any additional effort

with respect to the standard method, the technique requires the definition of a discretized space by assigning to each cell its own electromagnetic properties, which is not an easy process /15-18/. Specifically, the problems to be solved in SAR reduction need a correct representation of the cellular phone, anatomical representation of the head, alignment of the phone and the head, and suitable design of metamaterials.

In /12/,/19/ a perfect electric conductor (PEC) reflector was placed between a human head and the driver of a folded loop antenna. The result showed that the radiation efficiency can be enhanced and the peak SAR value can be reduced. In /15/, /20/ a study on the effects of attaching conductive materials to cellular phone for SAR reduction has been presented. It is shown that the position of the shielding material is an important factor for SAR reduction effectiveness. There is a necessity to make an effort for reducing the spatial peak SAR in the design stage of the ferrite sheet because the possibility of a spatial peak SAR exceeding the recommended exposure limit cannot be completely ruled out.

Metamaterials have inspired great interest due to their unique physical properties and novel application /14/, /21/. Metamaterials denote artificially constructed materials having electromagnetic properties not generally found in nature. Two important parameters, electric permittivity and magnetic permeability determine the response of the materials and metamaterials to electromagnetic fields. The negative permittivity can be obtained by arranging the metallic thin wires periodically /22-24/. On the other hand, an array of split ring resonators (SRRS) can exhibit negative effective permeability. The designed SRRS operated at 1.8 GHz and were used to reduce the SAR value in a lossy material. In /12/, the designed SRRS operated at 1.8 GHz were used to reduce the SAR value in a lossy material. The metamaterials are designed on circuit board so it may be easily integrated to the cellular phone. Simulation of wave propagation into metamaterials was proposed in /13/. The authors utilized the FDTD method with lossy-Drude models for metamaterials simulation. This method is a helpful approach to study the wave propagation characteristics of metamaterials /25/ and has been more developed with the perfectly matched layer (PML) and extended to three-dimension problem /26/.

At first materials are placed between the antenna and a human head, and then replaced by a metamaterial. In order to study the SAR reduction of an antenna operated at the GSM 900 band, the effective medium parameter of metamaterials is set to be negative at 900 MHz Different positions, sizes, and negative medium parameters of metamaterials for SAR reduction effectiveness are also analyzed.

This paper is structured as follows. Section II describes the numerical analysis of the handset together with the SAM phantom head, and the FDTD method is used with positive meshing techniques for quick and correct analysis. will be described in Section II. The SRRS structure, design and simulation of metamaterials results are explained in Section III, Section IV concludes the paper.

2. Simulation model and numerical techniques

A. Model Description

The simulation model which includes the handset with PIFA type of antenna and the SAM phantom head provided by CST Microwave Studio® (CST MWS) is shown in Fig. 1. A complete handset model composed of the circuit board, LCD display, keypad, battery, and housing was used for simulation. The relative permittivity and conductivity of individual components were set to comply with industrial standards. In addition, definitions in /5-6/, /20/ were adopted for material parameters involved in the SAM phantom head. In order to accurately characterize the performance over a broad frequency range, dispersive models for all the dielectrics were adopted during the simulation /5/. Fig. 2 shows the dispersive permittivity of the liquid in the SAM phantom head for simulation. In Fig. 2, Eps' and Eps'' represents dielectric dispersion fit Debye 1st order and 2nd order respectively. The electrical properties of materials used for simulation are listed in Table 1. A PIFA type antenna constructed in a helical sense operating at 900 MHz for GSM application was used in the simulation model. In order to obtain a high-quality geometry approximation for such a helical structure, a predictable meshing scheme used in the FDTD method usually requires large number of hexahedrons which in turn makes it extremely challenging to get convergent results within reasonable simulation time.

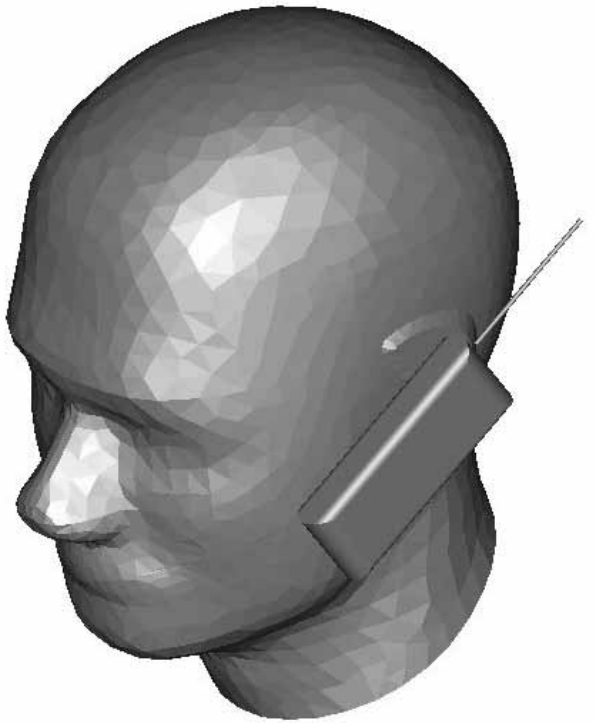

Fig. 1. Complete model used for simulation including handset and SAM phantom head.

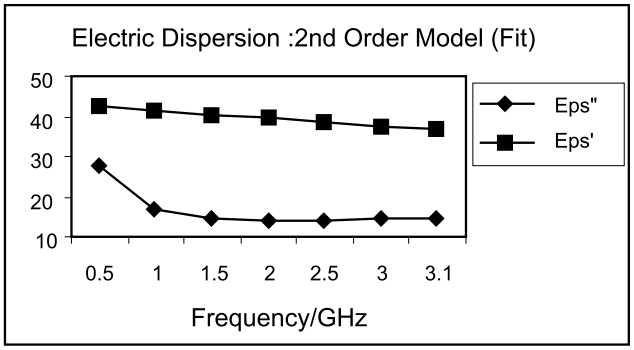

Fig. 2. Dispersive permittivity of the liquid in the SAM phantom head used for simulation.

Table 1: Electrical properties of materials used for simulation

Phone Materials	ε_r	σ(S/m)
Circuit Board	4.4	0.05
Housing Plastic	2.5	0.005
LCD Display	3.0	0.02
Rubber	2.5	0.005
SAM Phantom Head		
Shell	3.7	0.0016
Liquid @ 900MHz	40	1.42

B. Numerical Technique

CST MWS, based on the finite integral time-domain technique (FITD), was used as the main simulation instrument. A non-uniform meshing scheme was adopted so that the major computation endeavor was dedicated to regions along the inhomogeneous boundaries for fast and perfect analysis. Fig. 3 shows the mesh for two cut planes of the complete model indicating the area with denser meshing along the inhomogeneous boundaries. The minimum and maximum mesh sizes were 0.3 mm and 1.0 mm, respectively. A total of 2,097,152 mesh cells were generated for the complete model, and the simulation time was 1163 seconds (including mesh generation) for each run on an Intel Core™ 2 Duo E 8400 3.0 GHz CPU with 4 GB RAM system.

The analysis workflow started from the design of the antenna with complete handset model in free space. The antenna was designed such that the *S*11 response was less than -10 dB over the frequency band of interest. The SAM phantom head was then included for SAR calculation using the standard definition as /7/

$$SAR = \frac{\sigma}{2\rho} E^2 .$$

where *E* is the induced electric field (V/m), ρ is the density of the tissue (kg/m^3), and σ is the conductivity of the tissue (S/m). The resultant SAR values averaged over 1 gm and 10 gm of tissue in the head were denoted as SAR 1 gm and SAR 10 gm, respectively. These values were used as a benchmark to appraise the effectiveness in peak SAR reduction.

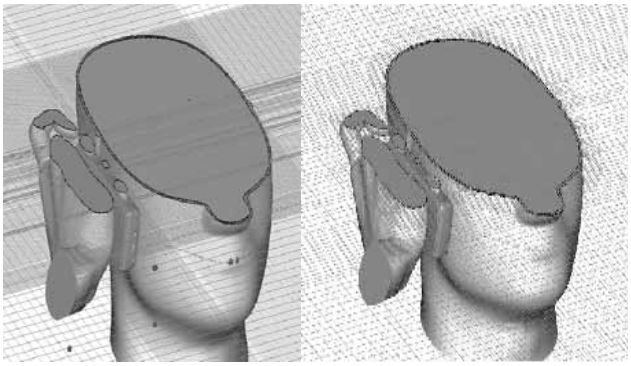

Fig. 3. Mesh view for two cut planes of the complete model showing the non-uniform meshing scheme adopted for simulation.

Fig. 4 shows a portable telephone model at 900 MHz for the present study. It was considered to be a quarter wavelength PIFA antenna mounted on a rectangular conducting box. The conducting box was 10 cm tall, 4 cm wide, and 3 cm thick. The PIFA antenna was located at the top surface of the conducting box.

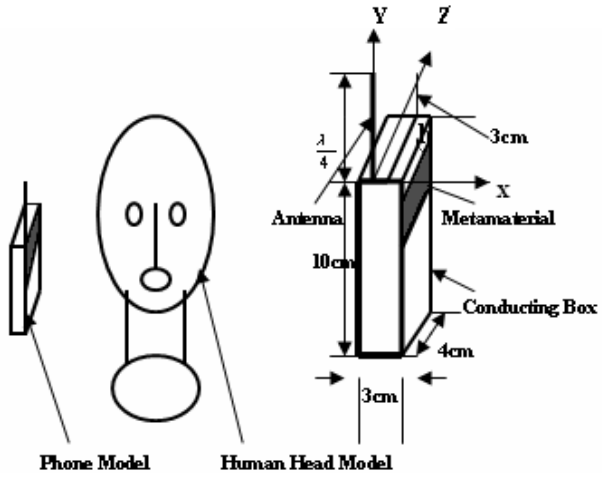

Fig. 4. The head and antenna model for SAR calculation.

The SAM head model was considered for this research where it consists about 2,097,152 cubical cells with a resolution of 1 mm. The FDTD method was employed in the numerical analysis. Its discretized formulations were derived from the following Maxwell's time-domain equations:

$$\frac{\delta H}{\delta t} = -\frac{1}{\mu_0 \mu_r'}(\nabla \times E) - \frac{\sigma^*}{\mu_0 \mu_r'} H. \quad (1)$$

$$\frac{\delta E}{\delta t} = -\frac{1}{\varepsilon_0 \varepsilon_r'}(\nabla \times H) - \frac{\sigma}{\varepsilon_0 \varepsilon_r'} E. \quad (2)$$

where $\sigma^* = \omega \mu_0 \mu_r'$ and $\sigma = \omega \varepsilon_0 \varepsilon_r''$ were added for treating magnetically and electrically lossy materials, respectively. A space domain enclosing the human head and the phone model is also shown in Fig. 5. The time step was set to $\frac{\delta}{\sqrt{3}c}$, where *c*

is the speed of light, to guarantee the numerical stability. The time-stepping was performed for about eight sinusoidal cycles in order to reach a steady state. To absorb the outgoing scattered waves, the second order Mur absorbing boundaries acting on electric fields were used. An antenna excitation was introduced by specifying a sinusoidal voltage across the one-cell gap between the helix and the top surface of the conducting box.

The antenna output power is defined as

$$P_{out} = P_{abs} + P_{ferr} + P_{rad}$$
$$= \frac{1}{2}\int_{Vh} \sigma |E|^2 \, dv + \frac{1}{2}\int_{Vf} (\sigma |E|^2 + \sigma^* |H|^2) \, dv$$
$$+ \frac{1}{2} \mathrm{Re}\left(\int_s E \times H^* . \vec{n} . ds\right) \quad (3)$$

where P_{abs} is the power absorbed in the head with a volume of V_h, P_{ferr} is the power dissipated in the ferrite sheet with a volume of V_f, and $P_{rad.}$ is the power radiated to the far-field, which can be calculated by integrating the normal component of the Pointing vector E x H^* over a surface S completely surrounding the head/phone model configuration.

3. Reduction of sar using metamaterial

The SAR in the head can be reduced by placing a metamaterial between the antenna and the human head. The metamaterial is on a scale less than the operating wavelength. The structures are resonant due to internal capacitance and inductance. The stop band can be designed at the operation bands of cellular phone radiation. The metamaterial are designed on a printed circuit board so it may be easily integrated to the cellular phone. By arranging sub-wavelength resonators periodically we get the metamaterial structure.

A. SRRS Structure

We establish that metamaterials can be used to reduce the peak SAR 1 gm and SAR 10 gm in the head from the FDTD analysis. In this section, metamaterials operated at the 900 and 1800 MHz bands of the cellular phone were considered. The metamaterials can be attained by arranging SRRS periodically. The SRRS structure consists of two concentric rings of conductive material. There is a gap on each ring, and each ring is situated opposite to the gap on the other ring. The schematics of the SRRS structure that we used in this study as shown in Fig. 6. The significant frequency of the SRRS can be varied toward a higher or lower frequency band by appropriately choosing these structure parameters.

B. SRRS Design

To construct the metamaterial for SAR reduction, we proposed one model of resonators namely the SRRS as shown in Fig. 6. We design the resonators for operation at the 900 MHz bands. The SRRS contains two square rings, each with gaps appearing on the opposite sides /14/. The SRRS was introduced by Pendry et al. in 1999 /16/ and subsequently used by Smith et al. for synthesis of the first left-handed artificial medium /21/. A lot of effort worldwide has been spent studying single negative metamaterials (SNMs), double negative metamaterials (DNMs), their properties /5-7/, /21/, applications in antennas /7/, /21–22/, and other microwave devices /21– 23/. In Fig. 6, the structures of resonators are defined by the following structure parameters: the ring thickness c, the ring gap d, the square ring size l, the split gap g, and c_0 is the speed of light in free space. The resonant frequency f is very sensitive to small changes in the structure dimensions of the SRRS. The frequency response can be scaled to higher or lower frequency by properly choosing these geometry parameters. After an extensive simulation study, we have found out a closed-form formula for the resonant frequencies of the SRRS:

$$f_{SRRS} = k_1 \frac{c_0}{2[4(2r_{ext} - c) - g]\varepsilon_r^{1/2}} \quad (4)$$

The SRRS is resonating at approximately half the guided-wavelength of the resonant frequency. There are two resonances from the split rings. We have given the formula for the resonance of the outer split ring, which has a lower resonance frequency.

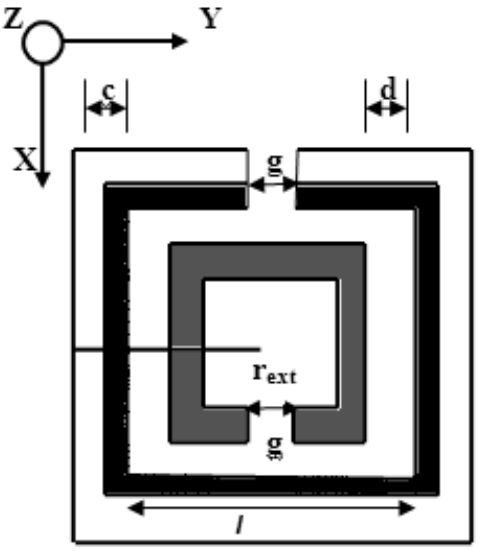

Fig. 6. The structure of the SRRS.

Numerical simulations that predict the transmission properties depend on the various structure parameters of this system. Simulations of this complex structure are performed with the FDTD method. To construct the resonators for SAR reduction, let us assume that the resonators lie in the *xz* plane, as shown in Fig. 7. The EM wave propagates along the *y* direction. The electric polarization is kept along the *z*-axis and magnetic field polarization is kept along *x* axis. Periodic boundary conditions are used to reduce the computational domain and an absorbing boundary condition is used at the propagation regions. The total-field/scatter-field formulation is used to excite the plane wave. The regions

inside of the computational domain and outside of the SRRS were assumed to be vacuum.

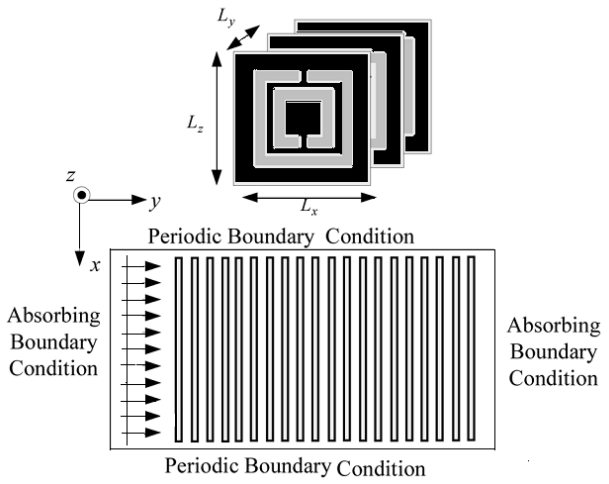

Fig. 7 Top view of a plane wave incident on the periodic (SRRS).

From this study, it is found that both of the two incident polarizations can produce a stop band. As shown in /23-26/, the stop band corresponds to a region where either the permittivity or permeability is negative. When the magnetic field is polarized along the split ring axes, it will produce a magnetic field that may either oppose or enhance the incident field. A large capacitance in the region between the rings will be generated and the electric field will be powerfully concentrated. There is strong field coupling between the SRRS and the permeability of the medium will be negative at the stop band. Because the magnetic field is parallel to the plane of SRRS, we imagine the magnetic effects are small, and that permeability is small, positive, and slowly varying. In this condition, these structures can be viewed as arranging the metallic wires periodically.

The stop bands of the SRRS are designed to be at 900 MHz and 1800 MHz. The periodicity along x, y, z axes are L_x = 63 mm, L_y = 1.5 mm, and L_z = 63 mm respectively. On the other hand, to obtain a stop band at 1800 MHz, the parameters of the SRRS are chosen as c = 1.8 mm, d = 0.6 mm, g = 0.6 mm, and r = 12.9 mm. The periodicity along the x, y, z axes are L_x = 50 mm, L_y = 1.5 mm, and L_z = 50 mm, respectively. Both the thickness and dielectric constant of the circuit boards for 900 MHz and 1800 MHz are 0.508 mm and 3.38 mm respectively. After properly choosing geometry parameters, the SRRS medium can display a stop band around 900 MHz and 1800 MHz. SRRS producing a good stop band and size are large. Therefore, SRRS are suitable for mobile phones as per size and recital point of view.

We have tried to use a high impedance surface configuration /22/ to reduce the peak SAR. However, we found that when these structures operate at 900 MHz, the sizes of these structures are too large for cellular phone application. A negative permittivity medium can also be constructed by arranging the metallic thin wires periodically /24/. However, we found that when the thin wires operate at 900 MHz, the size is also too large for practical application. Because the SRRS structures are significant due to internal capacitance and inductance, they are on a scale less than the wavelength of radiation. In this study, it is established that the SRRS can be designed at 900 MHz while the size is similar to that of a cellular phone.

Table 3: Comparisons of peak sar at 900 mhz without metamaterial

Tissue	SAR value (W/kg)
SAR value for /7/	2.17
SAR value for /14/	2.43
SAR value for /20/	2.28
SAR value this work for 1 gm	2.002

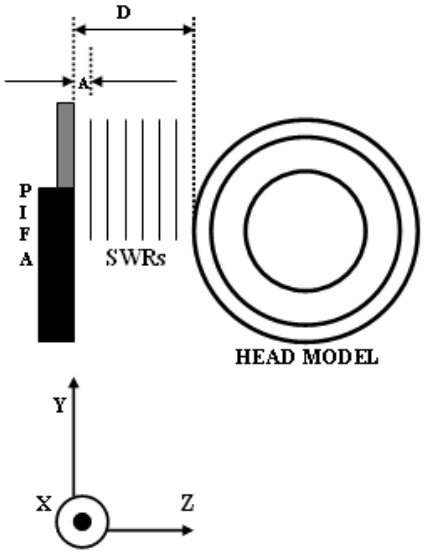

Fig. 8. The antenna, metamaterials, and head model for SAR reduction.

C. Results

The designed SRRS were placed between the antenna and the human head. Fig. 8 shows the head used in SAR simulation. The antenna was arranged parallel to the head axis. The distance between the antenna and head surface was 20 mm. The SAR value was calculated for an antenna output power equal to 600 mW. The calculated peak SAR 1 gm without metamaterials was 2.002 W/kg. The SAR simulation is compared with the results in /7/, /14/, /20/ for validation, as shown in Table III. The distance between the antenna feeding point and edge of the metamaterials was A= 3 mm. The size of the metamaterials in the *xz* plane was 48 mm × 48 mm and the thickness was 6 mm. The SAR value and antenna performance with the metamaterial were analyzed. To evaluate the power radiated from the antenna, the source impedance (Z_S) was assumed to be equal to the complex conjugate of the free space radiation impedance (Z_S= 102.14+ j83.78Ω). The source voltage (V_S) was chosen to obtain a radiated power in free space equal to 600 mW ($V_S = \sqrt{0.6.8.R_{R0}}$.). When analyzing the effect of

the metamaterials and the human head on the antenna performance, the source impedance and source voltage were fixed at the Z_S and V_S values. The power radiated from the antenna was evaluated by comparing the radiation impedance in this situation ($Z_R = R_R + jX_R$) and used the following /19/ equation:

$$P_R = \frac{1}{2} V_S^2 \frac{R_R}{|Z_R + Z_S|^2} \quad (5)$$

The total power absorbed in the head was calculated by

$$P_{abs} = \frac{1}{2} \int_V \sigma |E|^2 dv \quad (6)$$

Table 4: Effects of metamaterial on antenna performances and sar reduction at 900 mhz

	$Z_R(\Omega)$	P_R(mW)	P_{abs}(mW)	SAR 1 gm (W/Kg)
Without material	63.39+j94.53	600	268.83	2.002
μ= 1, ε= -3	51.93+j99.79	514.6	211.95	1.0897
μ= 1, ε = -5	54.12+j95.25	532.8	238.45	1.5635
μ= 1, ε = -7	59.25+j96.14	541.9	251.34	1.732

Different negative medium parameters for SAR reduction effectiveness were analyzed. We placed negative permittivity mediums between the antenna and the human head. First, the plasma frequencies of the mediums were set to be ω_{pe} = 9.309X10^9 rad/s, which give mediums with μ = 1 and ε = -3 at 900 MHz. The mediums with larger negative permittivity μ = 1, and ε = -5; μ = 1, and ε = -7 were also analyzed. We set Γ_e = 1.2 X 10^8 rad/s, suggesting the mediums have losses. Numerical results of SAR value and antenna performance are given in Table IV. The peak SAR 1 gm becomes 1.0897 W/kg with μ = 1 and ε = -3 mediums. Compared to the condition without metamaterials, the radiated power is reduced by 13.9% while the SAR is reduced by 53.35%. With the use of and mediums, the SAR reduction effectiveness is decreased. However, the radiated power from the antenna is less affected. Comparisons of the SAR reduction effectiveness with different positions and sizes of metamaterials were analyzed. Simulation results are shown in Table V. In case 1, the distance between the antenna and metamaterial was changed from 3 mm to 6 mm. In case 2, the metamaterial thickness was reduced from 6 mm to 3 mm. It is found that both the peak SAR 1 gm and power absorbed by the head increase with the increase of distance or the decrease of thickness. In case 3, the size of the metamaterial was increased from 48 mm X 48 mm to 56 mm X 56 mm. It can be noted that the peak SAR 1 gm is reduced significantly while the dreadful conditions on the radiated power due to metamaterial is insignificant. To further examine whether the metamaterial affected the antenna performance or not, the radiation pattern of the PIFA antenna with the μ = 1 and ε = -3 metamaterial was analyzed.

The use of metamaterials was also compared with other SAR reduction techniques. A PEC reflector and a ferrite material are commonly used in SAR reduction. The PEC reflector and ferrite sheet were analyzed. The relative permittivity and permeability of the ferrite sheet were ε =7.0-j0.58 and μ =2.83-j3.25, respectively. Numerical results are shown in Table VI. A PEC placed between the human head and the antenna is studied. It can be found that the peak SAR 1 gm is increased with the use of a PEC reflector. This is because the EM wave can be induced in the neighbor of a PEC reflector due to scattering. When the size of PEC sheet is small compared to the human head, the head will absorb more EM energy. Similar results of peak SAR increase with PEC placement were also reported in /14/. The use of a ferrite sheet can reduce the peak SAR 1 gm effectively. However, the degradation on radiated power from the antenna is also significant. In addition, compared to the use of a ferrite sheet, the metamaterials can be designed on the circuit board so they may be easily integrated to the cellular phone.

Table 5: Effects of sizes and positions of metamaterial on antenna performances and sar values

	$Z_R(\Omega)$	P_R(mW)	P_{abs}(mW)	SAR 1 gm (W/Kg)
Without material	63.39+j94.53	600	268.83	2.002
μ=1, ε =-3	51.93+j99.79	514.6	211.95	1.0897
Case 1	58.37+j95.35	539.4	253.53	1.6105
Case 2	62.19+j96.86	557.2	258.74	1.6893
Case 3	69.15+j107.38	573.33	216.83	1.2346

Table 6: Comparisons of sar reduction techniques with different materials

	$Z_R(\Omega)$	P_R(mW)	SAR 1 gm (W/Kg)
μ= 1, ε = -3	51.93+j99.79	514.6	1.0897
PEC reflector	66.83+j32.23	509.3	4.6803
Ferrite sheet	169.33+j153.69	519.3	1.043

To study the effect of SAR reduction with the use of metamaterials, the radiated power from the PIFA antenna with μ =1 and ε = -3 mediums was fixed at 600 mW. Numerical results are shown in Table VII. It is found that calculated SAR value at 900 MHz, without the metamaterial, is 2.002 W/kg for SAR 1 gm and with the metamaterial, the reduction of the SAR 1 gm value is 1.1917 W/kg. The reduction is 41.47%.

Table 7: Effects of comparisons with metamaterials on sar reduction (p_r = 0.5 w for 900 mhz)

	900MHz	
	Without material	μ =1, ε =-3
SAR 1 gm value for /14/	2.43	1.89
SAR 1 gm value in this work	2.002	1.1917

From simulation results, the metamaterials can reduce peak SAR effectively and the antenna performance can be less affected. The metamaterials are resonant due to internal capacitance and inductance. The mediums will display a stop band with a single negative medium parameter. Besides, we need to be more careful in taking the square root of negative

μ and ε of metamaterial. For example, instead of writing, $\varepsilon = -3$ we write $\varepsilon = 3 \exp(i\pi)$. When the mediums with $\mu = 1$ and $\varepsilon = -3$ are studied, the propagation constant becomes

$$\beta = \omega\sqrt{\mu\varepsilon\mu_0\varepsilon_0} = \omega\sqrt{3\mu_0\varepsilon_0} \times \exp(i\pi/2) = \omega\sqrt{3\mu_0\varepsilon_0} \quad (7)$$

The propagation constant is imaginary and the fields inside the metamaterials will fall off exponentially with the distance from the surface. Fig. 9 shows the simulated SAR distribution for an optimal metamaterial.

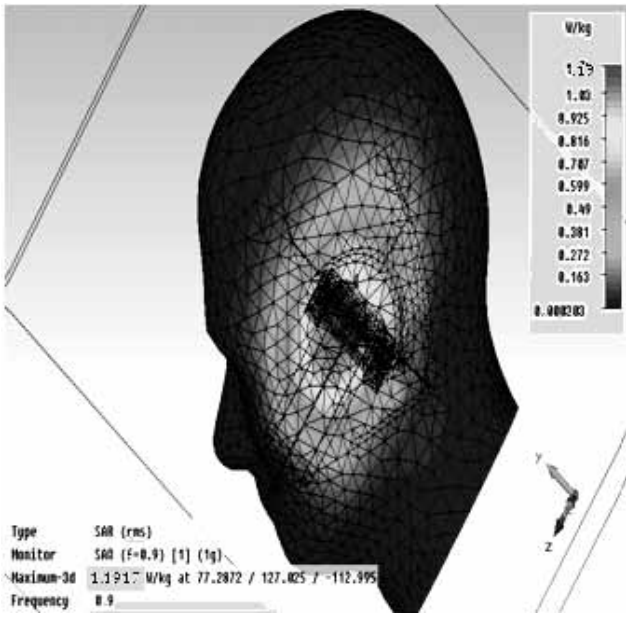

Fig. 9. SAR distributions after reduction using the metamaterial.

This work has achieved 41.47% of SAR reduction whereas the design reported in /14/ achieved 22.63% respectively. This is achieved due to the consideration of different density, different antenna, different size of metamaterial, different type of conductivity and it is because the electromagnetic source is being moved away from the head.

4. Conclusions

The EM absorption between an antenna and the human head with metamaterials has been discussed in this paper. Utilizing metamaterial in the phone model a SAR value is achieved of about 0.693 W/kg for SAR 10 gm and 1.1917 W/kg for SAR 1 gm is achieved. Based on the 3-D FDTD method with lossy-Drude model, it is found that for the both cases of peak SAR 1 gm and SAR 10 gm of the head can be reduced by placing metamaterials between the antenna and the human head. Numerical results can provide useful information in designing communication equipment for safety compliance.

Acknowledgement

The authors would like to thank Institute of Space Science (ANGKASA), Universiti Kebangsaan Malaysia (UKM) and the MOSTI Secretariat, Ministry of Science, Technology and Innovation of Malaysia, e- Science fund: 01-01-02-SF0566, for sponsoring this work.

References

/1/ Report of Telecommunications Technology Council for the ministry of Posts and Telecommunications, Deliberation no. 89, "Radio-Radiation Protection Guidelines for Human Exposure to Electromagnetic Fields," Tokyo, 1997.

/2/ K. S. Kunz and R. J. Luebbers, "The finite difference time domain method for electromagnetic," Boca Raton, FL, CRC, 1993.

/3/ IEEE C95.1-2005. "IEEE Standards for safety levels with respect to Human Exposure to Radio Frequency Electromagnetic fields,3KHz to 300GHz," Institute of Electrical and Electronics Engineers, Inc. New York, NY 2005.

/4/ International Non-Ionizing Radiation Committee of the International Radiation Protection Association, "Guidelines on Limits on exposure to radio frequency electromagnetic fields in the frequency range from 100KHz to 300GHz," Health Physics, vol.54 no. 1, pp. 115-123, 1988.

/5/ A. Hirata, T. Adachi, and T. Shiozawa, "Folded loop antenna with a reflector for mobile handsets at 2.0 GHz," Microwave Opt. Technol, Lett., vol.40, no.4, pp. 272-275, Feb. 2004.

/6/ A. Erentok, P. L. Luljak, and R. W. Ziolkowski, "Characterization of a volumetric metamaterial realization of an arti cial magnetic conductor for antenna applications," IEEE Trans. Antennas Propag., vol. 53, pp. 160–172, Jan. 2005.

/7/ J. Wang and O. Fujiwara, "FDTD computation of temperature rise in the human head for portable telephones," IEEE Trans. Microwave Theory Tech., vol. 47, no. 8, pp. 1528-1534, Aug.1999.

/8/ S. Curto, P. McEvoy, X. L. Bao, and M. J. Ammann, "Compact patch antenna for electromagnetic interaction with human tissue at 434 MHz," IEEE Trans. on Antennas and Propagation, vol. 57, no. 9, Sep. 2009.

/9/ J. Wang and O. Fujiwara, "Reduction of electromagnetic absorption in the human head for portable telephones by a ferrite sheet attachment," IEICE Trans. Commun., vol. E80b, no. 12, pp. 1810-1815, Dec. 1997.

/10/ K Kiminami, T Iyama, T Onishi, and S Uebayashi, "Novel specific absorption rate (SAR) estimation method based on 2-D scanned electric fields," IEEE Trans. on Electromagnetic Compatibility., vol. 50, no. 4, Nov. 2008.

/11/ R. G. Vaughan, and N. L. Scott, "Evaluation of Antenna Configurations for Reduced Power Absorption in the Head," IEEE Trans. On Vehicular Technology, vol. 48, no. 5, Sep. 1999

/12/ C. H. Li, N. Chavannes, and N. Kuster, "Effects of hand phantom on mobile phone antenna performance," IEEE Trans. On Antennas and Propagation, vol. 57, no. 9, Sep. 2009.

/13/ O. Kiverkas, J. Ollikainen, T. Lehtiniemi, and P. Vainikainen, "Bandwidth, SAR, and efficiency of internal mobile phone antennas," IEEE Trans. on Electromagnetic Compatibility., vol. 46, no. 1, Feb. 2004.

/14/ J. N. Hawang and Fu-chiarng chen. "Reduction of the peak SAR in the Human Head with Metamaterials" IEEE Trans. on antenna and propagation vol. 54 (12) 3763-3770, Dec. 2006.

/15/ L. C. Fung, S. W. Leung, and K. H. Chan, "Experimental study of SAR reduction on commercial products and shielding materials in mobile phone applications," Microwave and Optical Technology Letters, vol. 36, no. 6, pp. 419-422, March. 2003.

/16/ J. B. Pendry, A. J. Holen, D. J. Robbins, and W. J. Stewart, "Magnetism from conductors and enhanced nonlinear phenomena," IEEE Trans. Microwave Theory Tech., vol. 47, no. 11, pp. 2075–2084, Nov. 1999.

/17/ D. R .Smith, et al, "Composite medium with simultaneously negative permeability and permittivity," phys. Rev. Lett., vol. 84, no. 18, 4184-4187. , 2000.

/18/ G.F. Pedersen and J.B. Andersen, "Integrated antennas for hand-held telephones with low absorption", Proc. 44th IEEE Veh. Tech. Conf., Stockholm, Sweden, June. 1994, pp. 1537-1541.

/19/ R. Y. S. Tay, Q. Balzano and N. Kuster, "Dipole configuration with strongly improved radiation efficiency for hand-held transceivers", IEEE Trans. Antennas Propagat., vo1. 46, no. 6, pp. 798-806, June. 1998.

/20/ C .M .Kuo. and C. W. Kuo, "SAR distribution and temperature increase in the human head for mobile communication," in IEEE-APS Int. Symp. Dig., Columbus, OH, 2003, pp. 1025-1028

/21/ R. W. Ziolkowski, "Design, fabrication, and testing of double negative metamaterials," IEEE Trans. Antennas Propag., vol. 51, no. 7, pp. 1516–1529, Jul. 2003

/22/ D. R. Smith, D, R and Kroll, N. "Negative refractive index in left handed materials," phys. Rev. Lett., 85-14, 2933-2936, 2000

/23/ B. B. Beard, W. Kainz, T. Onishi, T. Iyama, S. Watanabe, O. Fujiwara, J. Wang, G. Bit-Babik, A. Faraone, J. Wiart, A. Christ, N.Kuster, A. Lee, H. Kroeze, M. Siegbahn, J. Keshvari, H. Abrishamkar, W. Simon, D. Manteuffel, and N. Nikoloski, " Comparisons of computed mobile phone induced SAR in the SAM phantom to that anatomically corrects model of the human head," IEEE Transaction on Electromagnetic Compatibility, vol. 48, no.2, pp 397-407, 2006.

/24/ M. M. Sigalalas ,C. T. Chan ,K .M. Ho ,and Soukoulis, "Metallic photonic band gap materials," Phys. Rev. B.,vol.52, no.16, pp. 11744-11760.

/25/ N. Engheta and R. W. Ziolkowski, "A positive future for double-negative metamaterials," IEEE Trans. Microwave Theory Tech., vol. 53, no. 4, pp. 1535-1556, Apr. 2005.

/26/ D. Correia and J. M. Jin, "3-D-FDTD-PML analysis of left-handed metamaterials," Microwave Optical Technol. Lett., vol. 40, no. 3, pp. 201-205, Feb. 2004.

Mohammad Rashed Iqbal Faruque[1],
Mohammad Tariqul Islam[2],
Norbahiah Misran[1, 2]

[1]Dept. of Electrical, Electronic and Systems Engineering, Faculty of Engineering and Built Environment, Universiti Kebangsaan Malaysia, 43600 UKM, Bangi, Selangor, Malaysia.

[2]Institute of Space Science (ANGKASA), Universiti Kebangsaan Malaysia, 43600 UKM, Bangi, Selangor, Malaysia.

rashedgen@yahoo.com,
titareq@yahoo.com,
bahiah@vlsi.eng.ukm.my

Prispelo: 06.02.2010 *Sprejeto: 24.06.2011*